Endogenous Electromagnetic Fields in Plant Leaves: A New Hypothesis for Vascular Pattern Formation

Alexis Mari Pietak, PhD

Department of Anatomy and Structural Biology, University of Otago, Dunedin, New Zealand

Email: alexis.pietak@gmail.com

Running title: Electromagnetic Fields in Leaf Vascularization

Keywords: Frohlich condensation, coherence domain, leaf vascularization, biological pattern formation

Abstract

Electromagnetic (EM) phenomena have long been implicated in biological development, but few detailed, practical mechanisms have been put forth to connect electromagnetism with morphogenetic processes. This work describes a new hypothesis for plant leaf veination, whereby an endogenous electric field forming as a result of a coherent Frohlich process, and corresponding to an EM resonant mode of the developing leaf structure, is capable of instigating leaf vascularisation. In order to test the feasibility of this hypothesis, a three-dimensional, EM finite-element model (FEM) of a leaf primordium was constructed to determine if suitable resonant modes were physically possible for geometric and physical parameters similar to those of developing leaf tissue. Using the FEM model, resonant EM modes with patterns of relevance to developing leaf vein modalities were detected. On account of the existence of shared geometric signatures in a leaf's vascular pattern and the electric field component of EM resonant modes supported by a developing leaf structure, further theoretical and experimental investigations are warranted. Significantly, this hypothesis is not limited to leaf vascular patterning, but may be applicable to a variety of morphogenetic phenomena in a number of living systems.

1. Introduction

1.1 Electromagnetism and Morphogenesis

While developmental biology has seen tremendous advances in the past few decades, there is much that remains to be understood. Most organisms embody rather precise and intricate organizations over a length scale roughly 10,000 times larger than the individual cells making up the organism. Plants, for instance, have been called living crystals on account of the mathematical intricacy implicit in the placement of their leaves/flowers/stems, and the patterns embodied by these individual parts (Jean 1996). Similarly, in the development of a mammalian limb, it remains to be understood how the length of bone segments, which follow mathematical relationships such as the Fibonacci sequence, are prescribed by developmental processes coordinating billions of cells in space and time. Modern developmental biology predominantly focuses on genetic, chemical, and mechanical mechanisms to account for various aspects of pattern formation in morphogenesis (Beloussov et al. 2006; Gilbert 2006; Koch et al. 1994). However, a significant (though rather neglected) body of research indicates that electromagnetic (EM) fields may play very important roles in the development and regeneration of a wide variety of organisms (Levin 2003; Nuccitelli 1992).

Due to their field-like characteristics, endogenous EM phenomena may be very capable of specifying information throughout a collective of cells to induce patterning over a large spatial range (Jerman et al. 2009). The theoretical possibility that structures commonly found in living systems could generate EM fields first arose from Frohlich in 1968 (Frohlich 1968; Frohlich 1975). Since dipolar molecules like water are attracted to one another by the Columbic force, a

collective of these molecules can be likened to a system of interconnected oscillators vibrating with thermal energy. Frohlich demonstrated that coherent vibration of a system of dipolar molecules could occur, and that this would generate an associated EM field (Frohlich 1968). These regions of synchronized vibrating molecules and associated EM field have since been referred to as *coherence domains* (Del Giudice et al. 1985). More recent advancements of Frohlich's ideas have used quantum field theory to expand upon the theory of endogenous EM fields in living systems (Arani et al. 1995; Brizhik et al. 2003; Cifra et al. 2009; Del Giudice et al. 2005; Del Giudice et al. 1985; Del Giudice et al. 1986; Del Giudice et al. 2009; Pokorny et al. 2005). The existence of coherence domains has been shown to critically depend on the open, dissipative, and far from thermodynamic equilibrium characteristics of living systems (Mesquita et al. 2005).

Models based on the Frohlich-effect predict endogenous EM fields in a frequency range between 10^9-10^{12} Hz (Cifra et al. 2009; Frohlich 1968). While the spatial dimensions of the range of coherent vibration and associated EM field have not been explicitly defined, it has been suggested that coherent, endogenous EM fields spanning distances relevant to individual cells, organs, and whole organisms are possible (Brizhik et al. 2009; Del Giudice et al. 2009). The polar oscillators have been speculated to be water molecules; charged, filamentous biomolecules; polar macromolecular structures such as the cell membrane; and even hierarchical assemblies of coherence domains (Brizhik et al. 2009; Cifra et al. 2009; Del Giudice et al. 2009; Jerman et al. 2009; Pokorny et al. 2005). Furthermore, while EM fields at microwave to terahertz frequencies would normally not persist due to the high dielectric loss characteristics of watery biological tissue (Fenske et al. 2000; Pethig 1987), the endogenous EM signals produced by a coherent

Frohlich-like process are theorized to be virtually non-dissipative (Mesquita et al. 1996; Mesquita et al. 2005).

A small number of reports provide experimental evidence of endogenous EM field formation in a variety of living systems. EM radiation at radio frequencies of 0.4-1.6 kHz (Cifra et al. 2008) and megahertz frequencies of 8-9 MHz (Pokorny et al. 2001) have been measured in yeast cultures. Non-thermal microwave emission has been reported from contracting frog legs (Gebbie et al. 1997). Additionally, there are many reports investigating EM emissions in the far infrared to ultraviolet range (biophotons, 10^{14}-10^{16} Hz) from a wide array of living organisms (Levin 2003; Popp et al. 2002; Popp et al. 2002; Van Wijk 1992; Van Wijk 2001; Van Wijk et al. 1992; Yan et al. 2005). Moreover, Popp's work with biophoton emission from plant leaves indicate the existence of a coherent endogenous EM field dependent on the integrity of the whole leaf tissue (Popp et al. 2002; Yan et al. 2005).

This work explores how EM fields arising from a Frohlich-like processes may be implicated in specific long-range morphogenetic patterning processes. On account of their ubiquitous presence in the everyday world, their two dimensional configuration which makes them easy to study, and their intricate patterns, this manuscript will specifically focus on the development of leaf vascular patterns.

1.2 Endogenous Electromagnetic Fields in Plant Leaves?

A leaf's veins arise spontaneously from a collective of self-same cells early in development (Scarpella et al. 2004; Ye 2002). The predominant mechanism proposed for leaf vein formation is the *auxin canalization hypothesis* (Mitchison 1980; Rolland-Lagan et al. 2005; Swarp et al. 2000; Uggla et al. 1996), whereby auxin exits cells with the assistance of auxin-efflux proteins

embedded in the cell membrane, in particular, a protein called PIN1. A positive feedback is thought to ensue as a cell conducting auxin preferentially expresses PIN1 at the membranes receiving more flux, further enhancing a cell's ability to transport auxin. Commitment of cells as an auxin channels leads to their differentiation into vascular tissue.

The auxin canalization hypothesis is supported by observations that disrupting auxin polarity or PIN1 expression in the early tissue development significantly disrupts leaf vascular pattern formation (Galweiler et al. 1998). Perhaps most significantly, the expression of PIN1 associated with auxin transport has been observed to reliably precede the observation of biological markers indicating cell differentiation towards vascular tissue (Scarpella et al. 2006). Mathematical models based on variations of efflux-protein mediated polar auxin transport have been put forth to describe the formation of linear veins spanning from auxin sources to sinks (Mitchison 1980), branched structures (Feugier et al. 2005), and closed-loops (Feugier et al. 2006) in leaf vasculature. Some have proposed auxin to be actively transported up concentration gradients to form discrete nodes consisting of high concentrations of auxin (Merks et al. 2007). However, while this combination of molecular mechanisms and feedback is believed to create a non-linear, dynamic system capable of forming leaf vascular patterns (Feugier et al. 2005), none of the current models can account for the long-range, mathematically described patterns that have been recently identified in dicotyledonous leaves (Pietak 2009). This of course does not necessarily make the auxin-canalization mechanisms or their variants inadequate, but merely leaves an opportunity for new mechanisms to be put forth.

The field of Synergetics engages the concept of *circular causality* to comprehend how the activity of light-producing atoms in a laser can become perfectly synchronized via a self-assembly process (Haken et al. 1995). Intrinsically, the laser cavity has EM resonant modes. While the

behaviour of light-producing atoms is initially desynchronized, as energy input into the open, dissipative system is increased, a resonant mode of the laser cavity is excited (Haken et al. 1995). The inherent impetus for the resonant mode to resonate is seen to 'enslave' the activity of the underlying light-producing atoms into perfect synchronization, and each atom produces light at the resonant frequency of the cavity with the same phase with respect to one another (Haken et al. 1995).

A similar process is envisaged for the formation of an endogenous EM field within developing leaf tissue. Leaves, like other biological tissues, are fairly strong dielectrics, with relative permittivities of ε_r=35-45 measured for fresh leaves (aspen and corn) at gigahertz frequencies (1-20 GHz) (El-Rayes et al. 1987). This means that any sustained EM field within the dielectric tissue should be subject to internal reflection due to the mismatch between the dielectric strength of the developing leaf and the surrounding environment (ε_r=1 for air, 80 for water). Thereby the leaf tissue, which is able to contain an EM field, can act as a resonant cavity akin to the resonant cavity of a laser. Thus, the dielectric leaf primordium also has naturally occurring EM resonant modes. If a Frohlich-like process generates a large coherence domain within the leaf primordium, this represents the coherent vibration of a number of dipolar oscillators, and will have an EM field associated with it. However, as in the case of the laser, the endogenous EM field must also correspond to an EM resonant mode of the developing leaf tissue. A tissue-wide coherent endogenous field would need to correspond to an EM resonant mode in order to satisfy boundary conditions, which is a key requirement of any physical system supporting any kind of system-wide vibration.

The spatially-patterned standing electric field component of an EM mode could then act on the developing leaf primordium in a manner dependent on the electric field strength and

direction. In regions of high electric field strength, an electric force may act on charged molecules, resulting in streaming currents or establishing cell polarity in the direction of the field. Alternatively, the electric field may act to turn on genes (for instance auxin expression) in a manner dependent on its strength. However, since dielectric loss tangents are also high in natural materials at microwave-terahertz frequencies (the loss tangent of mature fresh leaves at 8 GHz is approximately 0.25 (El-Rayes et al. 1987)), an endogenous EM field could only be sustained for a coherent Frohlich-like process with coherence spanning the entire range of the developing tissue (Mesquita et al. 1996; Mesquita et al. 2005).

Notably, the idea of a single cell acting as an EM resonator, and the resulting electric field influencing mitotic spindle arrangement in a dividing cell, was first introduced by Popp in 2005 (Popp et al. 2005).

2. Methods

2.1 Basic Rationale Directing the Model

Leaves form from leaf primordia, which in turn develop from undifferentiated meristematic tissue. The developing leaf bud consists of a nested set of leaves unfolding from the meristem. In general, leaf primordia have the following characteristics:

- Primary and secondary veins emerge from a previously homogeneous collection of meristematic cells which show no obvious distinctions before patterning occurs (Nelson et al. 1997).
- The primordium develops a central midvein early in development and prior to developing secondary veins (Klucking 1992; Nelson et al. 1997; Ye 2002).

- Secondary veins form while leaf structure is folded along the central midvein (personal observation, see Figure 1A).
- Primordia typically begin as narrow, pointed ellipses, even in leaves that develop a much different shape in maturity. Secondary veins tend to form while primordia are in this early state (personal observation, see Figure 1B and C).
- Primary and secondary veins develop in the leaf primordium and remain conserved in number in the mature leaf (Klucking 1992; Nelson et al. 1997; Ye 2002).
- The microwave dielectric constant of fresh, mature leaf tissue is between 25-45 and the conductivity is equal to or less than $1x10^{-6}$ S/m (El-Rayes et al. 1987).
- The size of the leaf primordium at the time of secondary vein development is between 2-9 mm in length, with a thickness of approximately 50-100 μm (personal observation from measurements of rose, horse chestnut, grape, oak, and apple leaves, also see Figure 1).

Therefore, the leaf primordium must be capable of supporting an electric field with a spatial configuration (for instance, the location and shape of maxima) in direct relation to the configuration of newly formed primary and/or secondary veins. This electric field must be able to form:

- In tissue with a dielectric constant of approximately ε_r=25-45 and a conductivity of approximately $1x10^{-6}$ S/m.
- In tissue shaped as a thin (approximately 50-100 μm thickness) narrow, pointed ellipse (see Figure 1).
- In tissue with electrical and geometrical properties similar to that of leaf tissue, which also contains a central midvein and is folded along the midvein.

- At frequencies of relevance to a Frohlich-like process: 10^9-10^{12} Hz.

2.2 Electromagnetic Finite Element Analysis Model

Three-dimensional, EM finite element modelling (FEM) software (Ansoft HFSS 11) was used to provide a primary assessment of the hypothesis by searching for resonant modes of material simulating the geometric and electrical properties of leaf primordia at EM frequencies relevant to the Frohlich-effect. Tetrahedral mesh elements were used in all models. Model meshes were created using the automatic adaptive meshing algorithms of the software. Model meshes varied between 15,000-35,000 elements depending on the model geometry, the size of the model, and the frequency of excitation. The EM resonant modes of various leaf primordium geometries were explored using the automated 'eigenmode analysis' routines of the FEM software, which finds resonant frequencies of the structure and the fields at those resonant frequencies.

Three basic geometric models were investigated: (i) model-A consisted of a thin pointed ellipse with length equal to three times the maximum width; (ii) model-B of a medium width, pointed ellipse with length equal to twice the maximum width; and (iii) model-C of a plump pointed ellipse (or circle) with length approximately equal to the maximum width. The basic form of each of these models are shown in Figure 2.

Model A, B, and C were constructed with initial lengths of 2 mm, widths prescribed by the respective model configuration, and initial thicknesses of 50 μm. The initial dielectric constant was set at ε_r=35, the conductivity at $1x10^{-6}$ S/m, and the dielectric loss tangent at zero.

The boundaries of the model leaf primordium were resistive with a value of $1x10^6$ Ohms/m. This set of dimensions and parameters will be referred to as the default model.

3. Results

The quality factor (Q-factor) represents a structure's capacity to sustain a vibration, where a higher Q-factor indicates a lower rate of energy loss and a longer vibration in response to an impulse. In an initial exploration, the Q-factor of the fundamental resonant mode for each structure was recorded as various model parameters were systematically changed. Thus, an assessment of the model leaf primodium's ability to support EM resonances could be obtained for a wide range of material parameters. The forms of the electric field component of this fundamental mode for each model are shown in the first row of Figure 2. The Q-factor of the fundamental mode was measured for (i) scaling the entire model (i.e. length, width, and thickness) by an integer multiplier from 0.5 to 20; (ii) altering the thickness/length ratio from 0.01 to 0.1; (iii) changing the dielectric constant from ε_r=5 to 50; (iv) changing the dielectric loss tangent from $1x10^{-5}$ to 0.5; and (v) changing the bulk conductivity from $1x10^{-8}$ to 4 S/m. For each free-parameter variation, the other parameters were fixed at values of the default model described above.

The results for this practice showed no change in the Q-factor of the fundamental mode with scaling of the entire model, however, the expected change in frequency of the fundamental mode resonance did occur with changing model size (data not shown). An approximately proportional decline in the Q-factor was seen for a decreasing thickness/length ratio (Figure 3A). Altering the dielectric constant resulted in a steady decrease in Q-factor of the resonant mode with decreasing ε_r (Figure 3B). The dielectric loss tangent exhibited a rather distinct transition

from high to low Q-factor at a value of approximately 0.01, with loss tangents above 0.01 indicating highly damped vibration (Figure 3C). A similar trend was noted for conductivity, with conductivities below 0.1 S/m supporting vibration and those exceeding 0.1 S/m markedly damped with low Q-factors (Figure 3D).

In a subsequent set of investigations, the first 11 resonant modes of the three default models were determined using the automated eigenmode analysis of the modelling software. Electric field direction of odd-numbered modes are plotted in Figure 2. Modes with field lines more or less parallel with the central axis (termed V-modes, as in Figure 2: mode 5 of model A and mode 9 of model B) were observed and are noted to be similar to the configuration of monocot veins. An alternative mode with electric field lines oriented perpendicular to the central axis (termed an H-mode, as in Figure 2: mode 3 of models A and B and mode 5 and 7 of model B) which is notably similar to the secondary vein structure of many dicotyledonous leaves, were also observed. In the circular model C, different modes consisting of high-field strength nodes located at the perimeter were primarily observed (termed N-modes, as in Figure 2 mode 5, 7 and 11 of model C). For all modes, the electric field direction lay tangential to the plane of the model leaf surface.

The geometry of the three models was scaled by a factor of 4 and the first 11 modes were again retrieved, only to find that the model scaled well to different sizes as similar mode configurations were returned.

The software was then used to return higher-order modes of the structures, which were found to have similar configurations to those of lower order modes (i.e. V- and H- modes were predominant in models A and B, while model C showed N-modes as well as other patterns). The Q-factors of modes increased significantly as mode number increased (Figure 4), with Model A

(thin pointed ellipse) having the highest Q-values, model C (pointed circle) the lowest, and Model B (medium pointed ellipse) intermediate values.

An example of a higher-frequency resonant H-mode (at f=61.3 GHz) is shown in Figure 5 for model-A with a length of 8 mm, thickness of 100 μm, and all other parameters equal to those of the default model. The electric field strength (Figure 5A), the electric field direction (Figure 5B), the expected currents in the volume coinciding with the electric field direction (Figure 5C), the side-view showing completely tangential electric field direction (Figure 5D), the side-view showing transverse magnetic field component (Figure 5E), and an actual leaf with a comparable secondary vein configuration to the electric field configuration for the resonant H-mode (Figure 5F) are shown as comprehensive details of the 61.3 GHz H-mode in model-A.

Figure 6 shows the electric field strength of modes for model B and C, both at a frequency of 50.4 GHz and sized to a length of 8 mm and a thickness of 100 μm. A resonant H-mode is shown in model B (Figure 6A) and an N-mode in model C (Figure 6C). The H-mode of model B consisted of periodic bands of high electric field strength with electric field in each of these bands directed perpendicular to the central axis, which was consistent with the H-mode obtained for model A at 61.3 GHz (see Figure 5). This configuration corresponds to patterning and flow direction of secondary veins in a number of dicotyledonous leaves (Figure 6B shows white ash, *Fraxinus Americana*, as a representative leaf). The N-mode of model C (Figure 6C) depicts a number of high electric field strength 'nodes' oriented about the perimeter, as well as a central pattern consisting of semi-circular bands of high electric field strength and field direction oriented tangential to the bands. If the field nodes were to form high levels of auxin, flow from these sources could create the large number of radial primary veins, while secondary veins could

form along the semi-circular bands, creating a structure with a comparable morphology to that of a leaf such as the North American waterlily, *Nymphaea odorata* (Figure 6D).

In order to better simulate the actual configuration of a developing leaf, a central cylinder with radius of 50 μm and length of 2 mm was added to the default models to simulate a midvein, and the model leaf blades were folded towards the middle along their central axis to angles (measured between the blades at the central axis) of 90°, 60°, and 20°. Repeating the eigenmode search for this new configuration showed no significant change in the form of the resulting modes, their Q-factors, and only small shifts in their resonant frequency, from unfolded counterparts. As an example, Figure 7 shows the electric field strength of the resonant modes forming in model A with blades folded at angles of 90° (Figure 7A), 60° (Figure 7B), and 20° (Figure 7C) along the central axis, in comparison to a rose leaf primordium (Figure 7E).

4. Discussion

The EM resonant modes of a thin slice of dielectric with shape, size, and electrical characteristics similar to those of leaf tissue have characteristics which may make them capable of directing secondary vein formation. Three different mode configurations, the V-mode, H-mode, and N-mode, were identified and explored in this work. The more narrow elliptical geometries of A- and B-models supported V- and H- modes, while the wider, circular model-C was the only to show N-modes. In all modes, the electric force field is oriented tangential to the plane of the leaf. In V-modes, field lines are oriented along, or at small angles to, the direction of the central axis in continuous bands, and share similarities with the parallel vein configurations of monocot leaves. In H-modes, electric field direction is perpendicular to the axial midvein, and bears resemblance to secondary vein orientation in dicotyledonous leaves. The field lines of H- and V-

modes could, hypothetically, move ions to establish currents, or establish cell polarity in a manner consistent with secondary vein formation in dicotyledonous leaves. The directional electric field could, for instance, be the symmetry breaking influence mandating a differential PIN1 expression on cell membranes resulting in cell polarity and channelled auxin flow. As an alternative mechanism, the N-mode, which contained nodes of high, localized electric field strength, could act on genetic expression of hormones such as auxin in areas of high field strength, thereby creating the previously observed nodes of high auxin concentration which are implicated in plant leaf veination (Aloni et al. 2003; Runions et al. 2005).

By examining changes to the Q-factor of the fundamental mode of the various models while altering key parameters, it was indicated that: (i) models showed similar behaviour under dimensional scaling; (ii) high dielectric strengths were ideal, with values below 5 failing to support an EM pattern; (iii) large thickness to length ratios were favourable, with thickness to length ratios below 0.01 failing to support EM patterns; (iv) low dielectric loss tangents were favourable with dielectric loss tangents exceeding values of 0.05 failing to support EM patterns, and (v) low conductivities were favourable with conductivities exceeding 1 S/m failing to support EM patterns. With the exception of dielectric loss tangents of 0.25, which are too high to support classical EM fields, leaf tissues have dielectric constants, thickness to length ratios, and conductivities appropriate for supporting resonant EM modes. The fact that dielectric loss tangents are too high is dismissed as endogenous fields are proposed to be the result of a tissue-wide coherent vibration of polar entities with a corresponding associated EM field, as discussed in the introduction (Engel et al. 2007; Mesquita et al. 1996; Mesquita et al. 2005).

Furthermore, similar patterns of electric field resonance were supported even when the leaf model included a central midvein and was significantly folded along the midvein. This

folded variation is important as it simulates the actual configuration of a developing leaf primordium (as shown in the example rose primordium of Figure 7E).

There are, however, discrepancies between the EM resonance modalities in the modelled leaf primordia and the form of actual leaf patterns. Most obviously, the electric field fronts in the model H-mode were found to be almost entirely perpendicular to the central axis with a linear shape, while in actual leaf primordia the secondary veins are oriented at an angle to the central midvein and are often curved in shape (compare the high electric field strength bands of the H-mode of Figure 5A with example leaf primordium in Figures 1B and 5F). This may be due to additional electrical features of the leaf, or because of limitations to the model itself.

There are several limitations of the modelling technique. Most notably, this whole investigation has focused on modelling classical EM resonances, which are proposed to arise from a Frohlich-like process described by quantum field theory. Also, the leaf tissue has been modelled as a homogeneous, continuous thin slice of material, when in reality, a leaf primordium is a highly heterogeneous, hierarchical, patterned substratum consisting of discrete but interacting cells with lipid membranes and organelles, extracellular matrix biopolymers such as cellulose, bound and unbound water (both of which exhibit very different EM behaviours where organically bound water is more similar to ice), and tissue systems composed of these elements in intricate pattern.

It is worth mentioning that coherent Frohlich processes have recently come under heavy criticism by theoretical modellers. Reimers et al (2009) have modelled a linear chain of tubulin-like oscillators intending to represent a microtubule, and have concluded that a strong and coherent Frohlich-like process cannot occur at temperatures of the physiological system (Reimers et al. 2009). However, quantum coherence has already been demonstrated in biological systems

(Del Giudice et al. 1989; Engel et al. 2007) and warm, wet, polymers (Collini et al. 2009). Moreover, the base model of Reimers et al has been criticised for being overly simplistic (Hammeroff 2010), as it consists of a linear chain of tubulin-like oscillators that do not represent true microtubule structure. In reality, microtubules are known to self-assemble into hollow cylinders comprised of 13 tubulin chains existing on a cylindrical lattice plane surface with an intricate 'Fibonacci geometry' (Dustin 1978). Models that have considered Frohlich coherence in a full microtubule model show Frohlich resonance (Samsonovich et al. 1992).

On account of the outcome of this modelling investigation, attempts to experimentally measure endogenous EM fields in the frequency range from about 20 to 300 GHz are warranted. It remains unclear if measurements of high frequency EM fields have ever even been attempted in plants, and therefore, no experimental evidence for the existence of microwave EM in plants currently exists. However, there is evidence that microwave and terahertz frequency radiation have significant effects on the growth and development of plants (Fedorov et al. 2003; Pietruszewski et al. 2007; Tafforeau et al. 2003). For example, flax seedlings exposed for two hours to a low-power (non-thermal), 105 GHz EM radiation source produced 10-20 epidermal meristems in the hypocotyls one month later (Tafforeau et al. 2003). Stimulating plant seeds with EM radiation (at a variety of frequencies from about 1-1200 GHz) increases the number of seeds that germinate, increases initial growth rates, and morphological features such as the number of root nodules (Fedorov et al. 2003; Pietruszewski et al. 2007). Stimulating rice plant embryos at 300 GHz lead to an increase in plant maturation, protein content, and morphological characteristics of the plant (Fedorov et al. 2003). Moreover, there is plenty of experimental evidence of basic electrical phenomena in plants, from diurnal potentials measured in plant leaves(Leach 1987; Parkinson et al. 1965) and tree trunks (Burr 1945; Burr 1947), to rapidly

propagating electrical signals relaying information in plant neural networks (Fromm et al. 2007; Spanswick 1971). Light, which is EM radiation at frequencies on the order of 10^{15} Hz (1000 THz) has also been implicated as a communication signal in plant growth, and experimental evidence suggests a coherent EM field at light frequencies exists in plant leaves (Popp et al. 2002; Popp et al. 2002; Yan et al. 2005). Plant tissue has also been shown to have the remarkable property of internally reflecting and transmitting light with low attenuation — a property similar to synthetic fibre optic cables (Mandoli et al. 1982). In conjunction with the results of this report, this substantial body of experimental work provides further justification for new experimental investigations of endogenous EM activity in plants.

5. Conclusions

In this work the hypothesis of electromagnetic fields in plant leaf veination has been described and explored using an electromagnetic finite element model. Resonant EM modes with geometric signatures plausibly related to leaf vascular pattern development were discovered in a model leaf primordium consisting of a thin slice of dielectric with similar electrical properties to actual leaf tissue. Resonant EM modes of similar format and Q-factor were possible in a more realistic model of the leaf primordium which included a central midvein and involved folding of the veins at the central axis.

The concept of tissue as an EM resonator stimulated by a Frohlich-like process need not be unique to plants, but due to the generic underpinnings of the proposed Frohlich-like process, could apply to a wide variety of situations in morphogenesis of many living things.

6. Acknowledgements

Many thanks to Prof Michael Sayer, Professor Emeritus of Physics at Queen's University in Kingston, Ontario, Canada, for many helpful discussions. Thanks to Dr. Jonathan Breeze of the Imperial College of London, for helpful discussions on electromagnetic finite element modelling of dielectric microwave resonators. Many thanks to Prof Igor Jerman of the Institute for Bioelectromagnetics and New Biology, Slovenia, for helpful comments and advice.

Figure Captions

Figure 1: Horse chestnut (*Aesculus hippocastanum*) leaves at various stages of development. Panel A shows the leaf at an early stage of development (length of 5.5 mm, scale bar shows 1 mm). The midvein has already formed (left side of image) and secondary veins are beginning to become visible. Leaf tissue is folded along the central midvein. Panel B shows an immature leaf (length 46 mm, scale bar shows 7 mm) in which secondary veins (approximately 16 are visible) have fully formed and the structure is unfolded. Panel C shows a mature leaf (length 230 mm, scale bar shows 33 mm) which has approximately the same number of secondary veins as the immature leaf (approximately 18 are visible).

Figure 2: Sampling of resonant mode morphologies for the first 11 modes of model A (left column), B (middle), and C (right column). The electric field direction is shown in each image. Resonant frequencies are listed in the lower right hand corner of each panel. Resonant modes were obtained for models 2 mm in length, 50 μm thick, ε_r=35, σ=1.6 μS/m, and tan∂=0.

Figure 3: Variation in Q-value of the fundamental mode of model C for systematic changes in base parameters. Panel A shows the effect of changing the model thickness/length ratio; panel B the effect of changing the relative dielectric constant; panel C the effect of changing the dielectric loss tangent; and panel D the effect of changing the model conductivity. The default model parameters were: length of 2 mm, thickness of 50 μm, dielectric constant of ε_r=35, conductivity of σ=1.6 μS/m, and dielectric loss tangent of tan∂=0.

Figure 4: Q-values of modes increase significantly as mode number increases. Model A (thin pointed ellipse) has the highest Q-values while model C (circle) has the lowest.

Figure 5: Eigenmode analysis derived H-mode at 61.3 GHz for model-A. Panel A shows electric field magnitude (legend shows red as highest and blue as lowest field strength), panel B shows electric field direction, panel C shows currents in volume, panel D shows electric field direction in side view, panel E the magnetic field direction in side view. Panel F shows a rhododendron leaf as a comparable secondary vein configuration.

Figure 6: Electric field strength of resonant modes for model B and C. Panel A shows the H-mode of model B at f=50.4 GHz, while Panel B shows a leaf (white ash) with a comparable morphology to an H-mode. Panel C shows the N-mode of model C at f=50.4 GHz, and a leaf (North American waterlily) with a comparable morphology is shown in Panel D. Coloured bar indicates the colour-map legend where red represents highest field strength and blue the lowest.

Figure 7: Electric field strength of the resonant mode at 61.3 GHz forming in model A with blades folded along the central axis. Panel A shows the front view of the resonant mode for an angle of 90^{o} between the blades, while panel B shows the front view for an angle of 60^{o}. Panels C and D show the front and side views of the resonant mode for a structure with only 20^{o} between the blades. Panel E shows the side-view of a rose leaf primordia for comparison. Legend to the left of each panel shows red as highest field strength and blue the lowest.

Figures

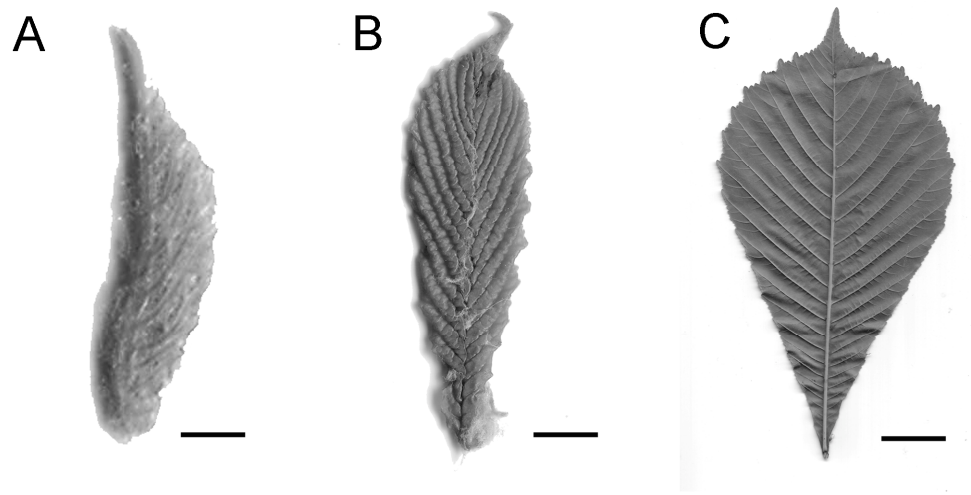

Figure 1

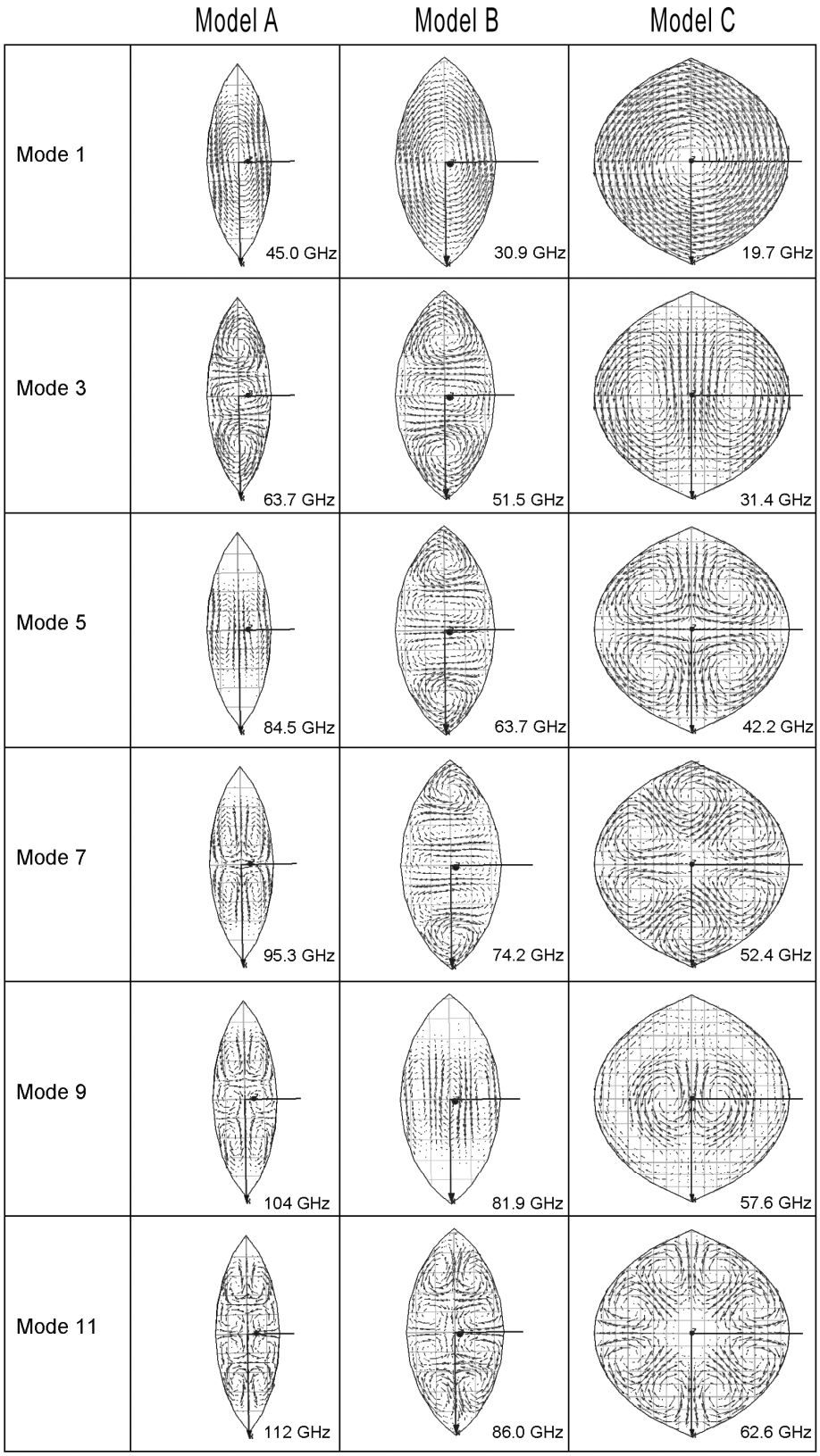
Model A
Model B
Model C
Mode 1
45.0 GHz
30.9 GHz
19.7 GHz
Mode 3
63.7 GHz
51.5 GHz
31.4 GHz
Mode 5
84.5 GHz
63.7 GHz
42.2 GHz
Mode 7
95.3 GHz
74.2 GHz
52.4 GHz
Mode 9
104 GHz
81.9 GHz
57.6 GHz
Mode 11
112 GHz
86.0 GHz
62.6 GHz

Figure 2

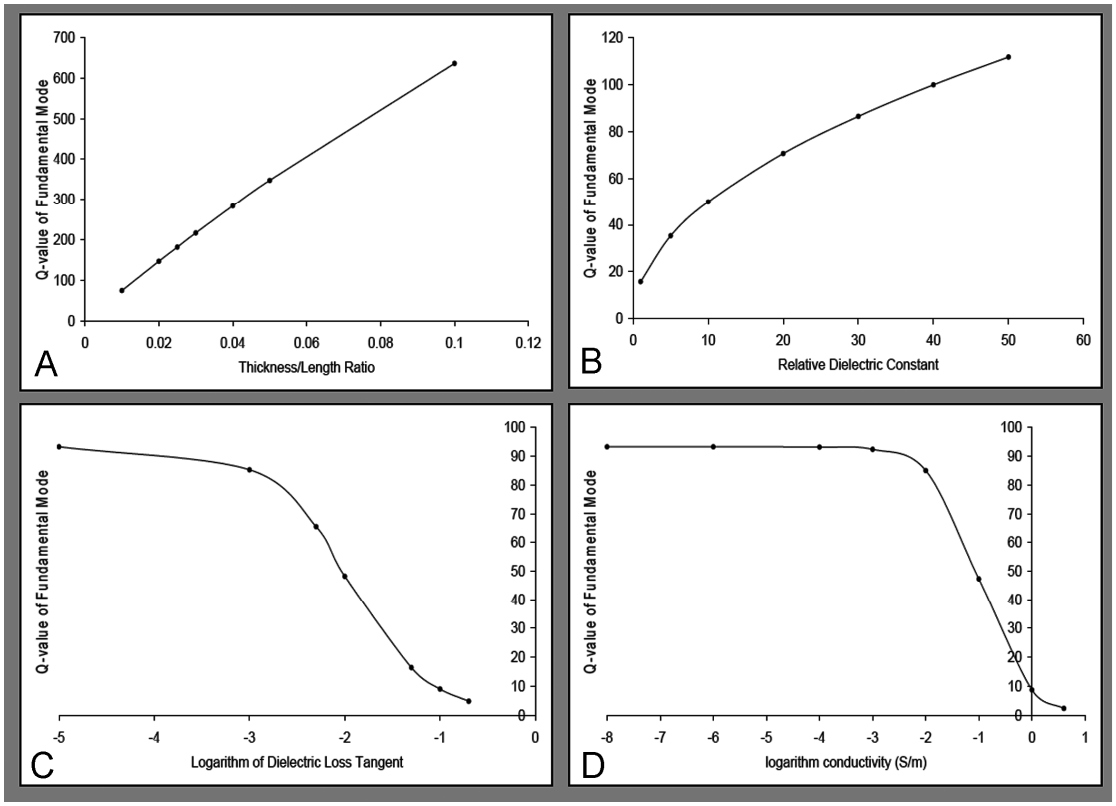
Q-value of Fundamental Mode
Thickness/Length Ratio
A
Q-value of Fundamental Mode
Relative Dielectric Constant
B
Q-value of Fundamental Mode
Logarithm of Dielectric Loss Tangent
C
Q-value of Fundamental Mode
logarithm conductivity (S/m)
D
Figure 3

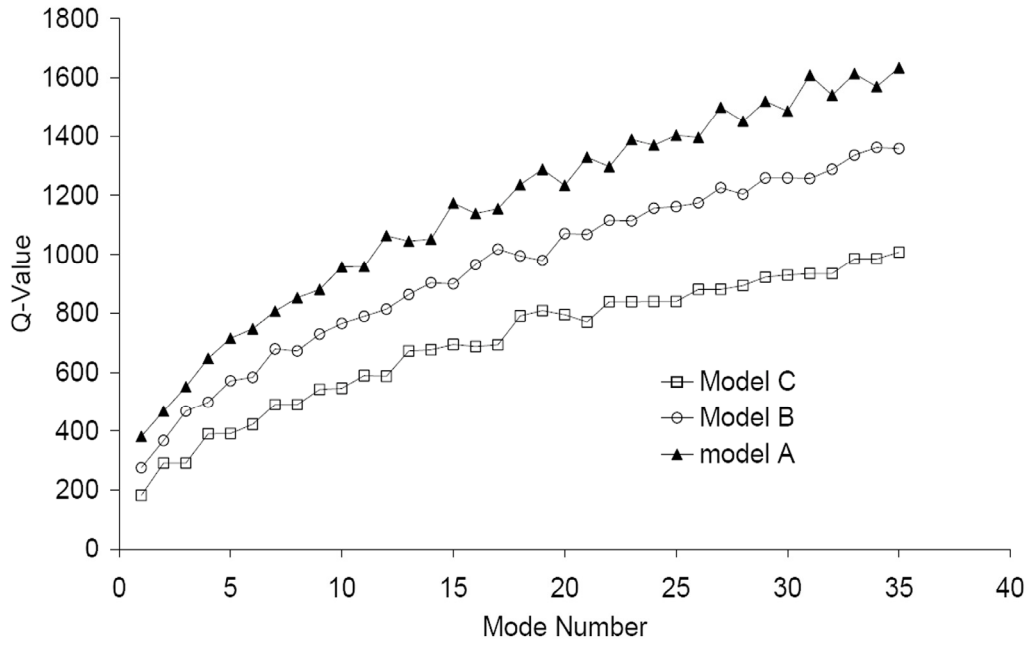
1800
1600
1400
1200
1000
800
600
400
200
0
Q-Value
0
5
10
15
20
25
30
35
40
Mode Number
Model C
Model B
model A

Figure 4

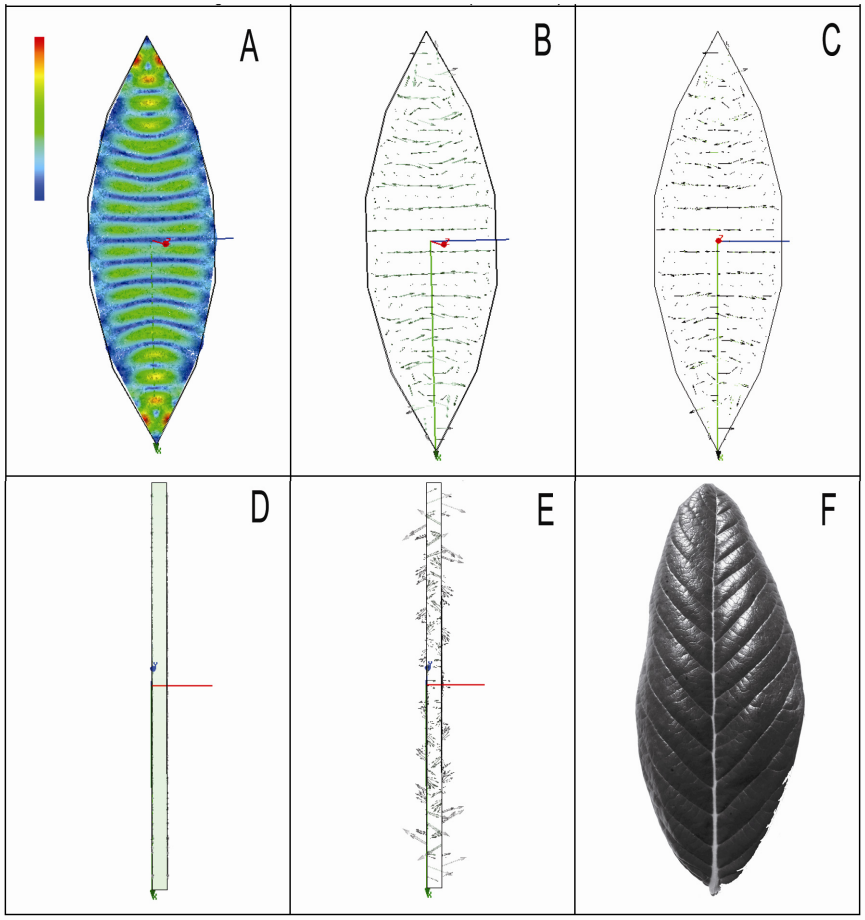

Figure 5

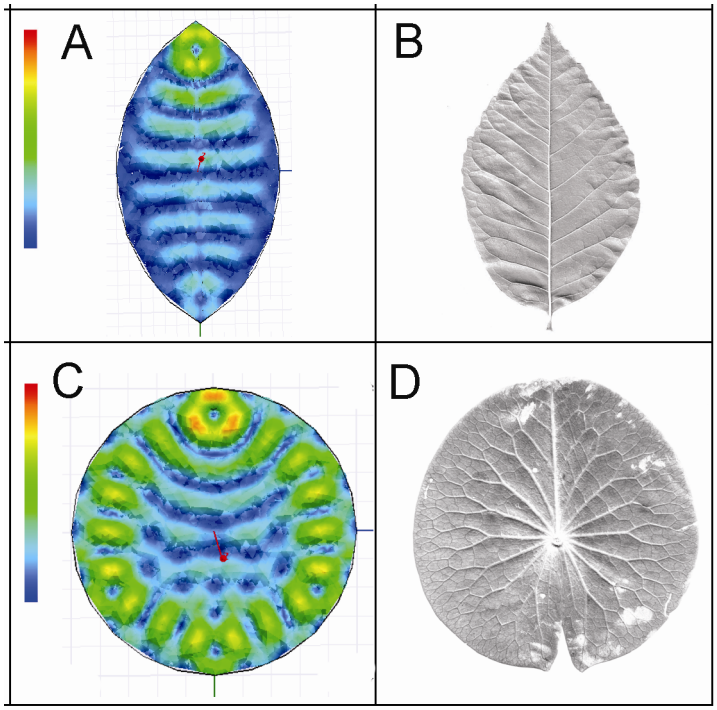

Figure 6

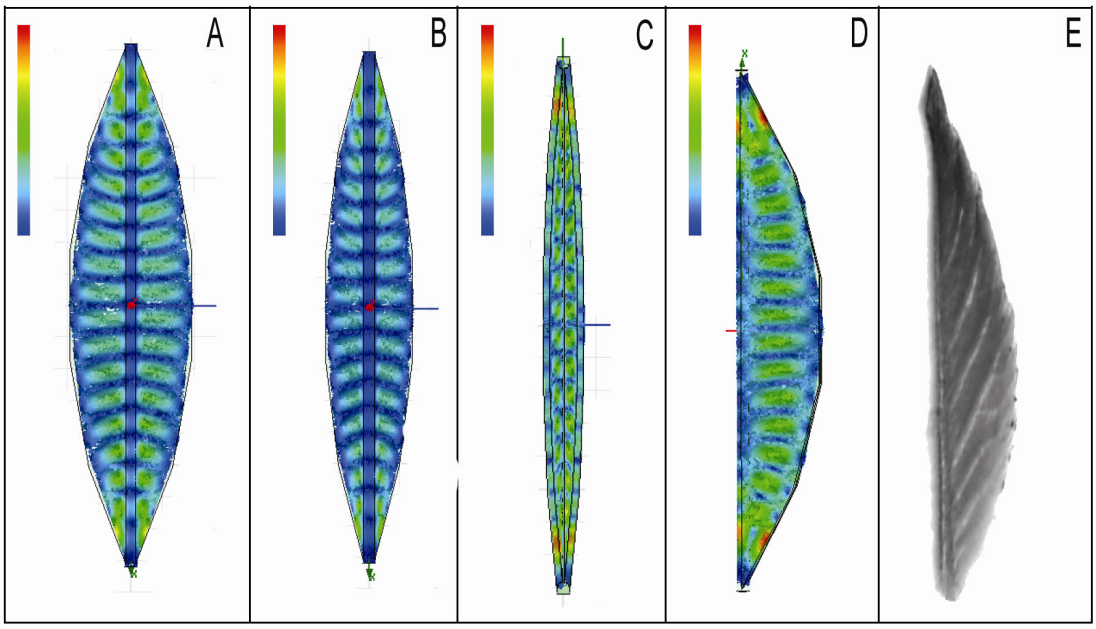

Figure 7

References

Aloni, R, Schwalm, K, Langhans, M and Ullrich, C (2003) Gradual shifts in sites of free-auxin production during leaf-primordium development and their role in vascular differentiation and leaf morphogenesis in Arabidopsis. *Planta* 216:841-853

Arani, R, Bono, I, Del Giudice, E and Preparata, G (1995) QED coherence and the thermodynamics of water. *Int J of Modern Physics B* 9:1813-1841

Beloussov, L and Grabovsky, V (2006) Morphomechanics:goals, basic experiments and models. *Int J Dev Biol* 50:81-92

Brizhik, L, Del Giudice, E, Jorgensen, S, Marchettini, N and Tiezzi, E (2009) The role of electromagnetic potentials in the evolutionary dynamics of ecosystems. *Ecological Modelling* 220:1865-1869

Brizhik, L, Del Giudice, E, Popp, F, Maric-Oehler, W and Schlebusch, K (2009) On the dynamics of self-organization in living organisms. *Electromagnetic Biology and Medicine* 28:28-40

Brizhik, L and Eremko, A (2003) Nonlinear model of the origin of endogenous alternating electromagnetic fields and selfregulation of metabolic processes in biosystems. *Electromagnetic Biology and Medicine* 22:31-39

Burr, H (1945) Diurnal potentials in the maple tree. *Yale J Biol Med* 17:727-734

Burr, H (1947) Tree potentials. *Yale J Biol Med* 19:311-318

Cifra, M, Pokorny, J, Jelinek, F and Hasek, J (2008). Measurement of yeast cell electrical oscillations around 1 kHz. PIERS Proceedings. Cambridge, USA**:** 780-785.

Cifra, M, Pokorny, J, Jelinek, F and Kucera, O (2009). Vibrations of electrically polar structures in biosystems give rise to electromagnetic field: theories and experiments. PIERS Proceedings. Moscow, Russia**:** 138-142.

Collini, E and Scholes, G (2009) Coherent intrachain energy migration in a conjugated polymer at room temperature. *Science* 323:369-373

Del Giudice, E, De Ninno, A, Fleischmann, M, Mengoli, G, Milani, M, Talpo, G and Vitiello, G (2005) Coherent quantum electrodynamics in living matter. *Electromagnetic Biology and Medicine* 24:199-210

Del Giudice, E, Dogila, S, Milani, M, Smith, C and Vitiello, G (1989) Magnetic flux quantization and Josephson behaviour in living systems. *Physica Scripta* 40:786-791

Del Giudice, E, Doglia, S and Milani, M (1985) Quantum field theoretical approach to the collective behaviour of biological systems. *Nuclear Physics B* B251:375-400

Del Giudice, E, Doglia, S and Milani, M (1986) Electromagnetic field and spontaneous symmetry breaking in biological matter. *Nuclear Physics B* B275:185-199

Del Giudice, E, Pulselli, R and Tiezzi, E (2009) Thermodynamics of irreversible processes and quantum field theory: an interplay for the understanding of ecosystem dynamics. *Ecological Modelling* 220:1874-1879

Dustin, P (1978) *Microtubules*. Springer-Verlag

El-Rayes, M and Ulaby, F (1987) Microwave dielectric spectrum of vegetation - part I: experimental observations. *IEEE Trans Geosci Remote Sens* GE-25:541-549

Engel, G, Calhoun, T, Read, E, Ahn, T, Mancal, T, Cheng, Y, Blankenship, R and Flemming, G (2007) Evidence for wavelike energy transfer through quantum coherence in photosynthetic systems. *Nature* 446:782-786

Fedorov, V, Popova, S and Pisarchik, A (2003) Dynamic effects of submillimeter wave radiation on biological objects of various levels of organization. *Int J Infared and Millimeter Waves* 24:1235-1254

Fenske, K and Misra, D (2000) Dielectric materials at microwave frequencies. *Applied Microwave Wireless* 12:92-100
Feugier, F and Iwasa, Y (2006) How canalization can make loops: A new model of reticulated leaf vascular pattern formation. *J Theor Bio* 243:235-244
Feugier, F, Mochizuki, A and Iwasa, Y (2005) Self-organization of the vascular system in plant leaves: Inter-dependent dynamics of auxin flux and carrier proteins. *J Theor Bio* 236:366-375
Frohlich, H (1968) Bose condensation of strongly excited longitudinal electric modes. *Physics Letters A* 26A:402-403
Frohlich, H (1968) Long-range coherence and energy storage in biological systems. *International J of Quantum Chemistry* 2:641-649
Frohlich, H (1975) Evidence for bose condensation-like excitation of coherent modes in biological systems. *Physics Letters A* 51A:21-22
Fromm, J and Lautner, S (2007) Electrical signals and their physiological significance in plants. *Plant, cell, and Environment* 30:249-257
Galweiler, L, Guan, C, Muller, A, Wiseman, E and Mendgen, K (1998) Regulation of polar auxin transport by AtPIN1 in Arabidopsis vascular tissue. *Science* 282:2226-2230
Gebbie, H and Miller, P (1997) Nonthermal microwave emission from frog muscles. *Int J Infared and Millimeter Waves* 18:951-957
Gilbert, S (2006) *Developmental Biology*. Sinauer Associates New York
Haken, H, Wunderlin, A and Yigitbasi, S (1995) An introduction to synergetics. *Open Systems and Information Dynamics* 3:97-130
Hammeroff, S. (2010). "Microtubule super-lattices, Frohlich coherence and ORch OR (Reply to Reimers et al, PNAS)." from www.quantumconsciousness.org/PNAS.html.
Jean, R (1996) Phyllotaxis: The status of the field. *Mathematical biosciences* 127:181-206
Jerman, I, Krasovec, R and Leskovar, R (2009) Deep significance of the field concept in contemporary biomedical sciences. *Electromagnetic Biology and Medicine* 28:61-70
Klucking, E (1992) *Leaf Venation Patterns*. J Cramer Berlin
Koch, A and Meinhardt, H (1994) Biological pattern formation: from basic mechanisms to complex structures. *Reviews Mod Phys* 66:1481-1494
Leach, C (1987) Diurnal electrical potentials of plant leaves under natural conditions. *Environment Experiment Botany* 27:419-430
Levin, M (2003) Bioelectromagnetics in Morphogenesis. *Bioelectromagnetics* 24:295-315
Mandoli, D and Briggs, W (1982) Optical properties of etiolated plant tissues. *PNAS* 79:2902-2906
Merks, R, Van de Peir, Y, Inze, D and Beemster, G (2007) Canalization without flux sensors: a travelling wave hypothesis. *Trends in Plant Sci* 12:384-389
Mesquita, M, Vasconcellos, A and Luzzi, R (1996) Near-dissipationless coherent excitations in biosystems. *Int J Quant Chem* 60:689-697
Mesquita, M, Vasconcellos, A, Luzzi, R and Mascarenhas, S (2005) Large-scale quantum effects in biological systems. *Int J Quant Chem* 102:1116-1130
Mitchison, T (1980) A model for vein formation in higher plants. *Proc Royal Soc London B - Bio Sci* 207:79-109
Nelson, T and Dengler, N (1997) Leaf vascular pattern formation. *Plant Cell* 9:1121-1135
Nuccitelli, R (1992) Endogenous ionic currents and DC electric fields in multicellular animal tissues. *Bioelectromagnetics* S1:147-157
Parkinson, K and Banbury, G (1965) Bio-electric potentials of intact green plants. *J Expt Botany* 17:297-308
Pethig, R (1987) Dielectric properties of body tissues. *Clin Phys Physiol Meas* 8:5-12

Pietak, A (2009) Describing long-range patterns in leaf vasculature with metaphoric fields. *J Theoretical Biology* 261:279-289

Pietruszewski, S, Muszynski, S and Dziwulska, A (2007) Electromagnetic fields and electromagnetic radiation as non-invasive external stimulants for seeds (selected methods and responses). *Int Agrophysics* 21:95-100

Pokorny, J, Hasek, J and Jelinek, F (2005) Endogenous electic field and organization of living matter. *Electromagnetic Biology and Medicine* 24:185-197

Pokorny, J, Hasek, J, Jelinek, F, Saroch, J and Palan, B (2001) Electromagnetic activity of yeast cells in the M phase. *Electro and Magnetobiology* 20:371-396

Popp, F, Chang, J, Herzog, A, Yan, Z and Yan, Y (2002) Evidence of non-classical (squeezed) light in biological systems. *Physics Letters A* 293:98-102

Popp, F, Walburg, M, Schlebusch, K and Klimek, W (2005) Evidence of light piping (meridian-like channels) in the human body and nonlocal emf effects. *Electromagnetic Biology and Medicine* 24:359-374

Popp, F and Yan, Y (2002) Delayed luminescence of biological systems in terms of coherent states. *Physics Letters A* 293:93-97

Reimers, J, Mckemmish, L, McKenzie, R, Mark, A and Hush, N (2009) Weak, strong, and coherent regimes of Frohlich condensation and their applications to terahertz medicine and quantum consciousness. *PNAS* 106:4219-4224

Rolland-Lagan, A and Prusinkiewicz, P (2005) Reviewing models of auxin canalization in the context of leaf vein pattern formation in Arabidopsis. *The Plant J* 44:854-865

Runions, A, Fuher, M, Lane, B, Federl, P, Rolland-Lagan, A and Prusinkiewicz, P (2005) Modeling and visualization of leaf veination patterns. *ACM Trans Graphics* 24:702-711

Samsonovich, A, Scott, A and Hameroff, S (1992) Acousto-conformational transitions in cytoskeletal microtubules: Implications for intracellular information processing. *Nanobiology* 1:457-468

Scarpella, E, Marcos, D, Triml, J and Berleth, T (2006) Control of leaf vascular patterning by polar auxin transport. *Genes and Development* 20:1015-1027

Scarpella, E and Meijer, A (2004) Pattern formation in the vascular system of monocot and dicot plant species. *New Phytologist* 164:209-242

Spanswick, R (1971) Electrical coupling between cells of higher plants: A direct demonstration of intercellular communication. *Planta* 102:215-227

Swarp, R, Marchant, A and MJ, B (2000) Auxin transport: Providing a sense of direction during plant development. *Biochem Soc Trans* 28:481-485

Tafforeau, M, Verdus, M, Norris, V, White, G, Cole, M, Demarty, M, Thellier, M and Ripoll, C (2003) Plant sensitivity to low intensity 105 GHz electromagnetic radiation. *Bioelectromagnetics* 00:1-5

Uggla, C, Moritz, T, Sandberg, G and Sundberg, B (1996) Auxin as a positional signal in pattern formation in plants. *PNAS* 93:9282-9286

Van Wijk, R (1992) Biophoton emission, stress and disease. *Experientia* 48:1029-1030

Van Wijk, R (2001) Bio-photons and bio-communication. *J Scientific Exploration* 15:183-197

Van Wijk, R and van Aken, J (1992) Photon emission in tumor biology. *Experientia* 48:1092-1103

Yan, Y, Popp, F, Sigrist, S, Sclesinger, D, Dolf, A, Yan, Z, Cohen, S and Chotia, A (2005) Further analysis of delayed luminescence of plants. *J Photochemistry and Photobiology B* 78:235-244

Ye, Z (2002) Vascular tissue differentiation and pattern formation in plants. *Annu Rev Plant Bio* 53:183-202